A Comparison of High-Fidelity Simulation Approaches for Interactional Aerodynamics of Multirotor Systems in Forward Flight

Abhishek Chopra	Richard Healy	Farhan Gandhi	Onkar Sahni
chopra3@rpi.edu	healyr@rpi.edu	fgandhi@rpi.edu	sahni@rpi.edu
PhD Student	PhD Student	Professor	Associate Professor

Center for Mobility with Vertical Lift (MOVE)
Rensselaer Polytechnic Institute, New York, USA

ABSTRACT

Recent advancements in distributed electric propulsion for urban air mobility applications have made interactional aerodynamics more common on modern rotorcraft designs. Rotor-to-rotor interactions are associated with complex flow features, and require high-fidelity numerical tools for adequate analysis and prediction. The computational cost associated with resolving these aerodynamic interactions can become prohibitively expensive, particularly when simulations over a multitude of operating conditions/configurations are desired. As an alternative to the typical blade-resolved DDES (BR-DDES) approach, an actuator line model with LES (ALM-LES) is considered for its high fidelity aerodynamic prediction capabilities at a reduced computational cost. In this study, flow field and rotor performance predictions using ALM-LES are compared to BR-DDES in order to evaluate the merits of ALM-LES for interactional aerodynamic analysis. Overall, the wake structure of the two-rotor system shows good agreement between the two methods. Integrated thrust is also predicted similarly, with a difference of 2.4% for the front rotor and 4.3% for the aft rotor. While integrated thrust is predicted well by ALM-LES, some discrepancies in sectional thrust are observed in areas with blade-vortex interaction (BVI). The vortex position compares well between the two methods, so the sectional thrust difference is tied to differences in vortex strength and how well ALM is able to represent a BVI. Sectional thrust differences are also observed on the aft rotor and are associated with secondary vortices convecting into the rotor plane. Despite differences in parts of the rotor disk with BVI, ALM-LES is shown to be capable of predicting the interactional aerodynamics of a two-rotor system in forward flight at about 1% the computational cost of BR-DDES.

INTRODUCTION

With the rise of electric vertical take-off and landing (eVTOL) aircraft for urban air mobility (UAM), the rotorcraft community is interested in multi-rotor designs due to the flexibility afforded by distributed-electric propulsion. Due to the relatively low energy density of current batteries it is important to maximize the aerodynamic performance of eVTOLs to realize practical payload capacity, endurance, and range. Computational fluid dynamics (CFD) is a valuable tool for predicting the complex aerodynamic interactions that arise between rotors operating in close-proximity. A computational tool that can accurately predict these interactions is particularly important, for example, to simulate non-axial flight conditions such as forward flight, where rotor blades encounter tip vortices both from preceding blades and from nearby rotors.

Such complex and unsteady aerodynamics require high-fidelity CFD such as large eddy simulation (LES) or detached eddy simulation (DES) to accurately capture the highly turbulent vortical flow generated around the rotor and in the wake. The issue with such high-fidelity simulations is that they are computationally expensive when the blade geometry is fully resolved (i.e., with a body-fitted mesh) and hence remains prohibitive for parametric design exploration, optimization, and uncertainty quantification. To remedy this situation, actuator models have been previously proposed for rotorcraft and wind-turbine flow field prediction. In any actuator model, which can include actuator disc model (ADM), actuator line model (ALM), or actuator surface model (ASM) (Ref. 1), the rotor blades are not explicitly represented in the computation and instead implicitly represented or modeled based on body force or momentum source terms. The forces in an actuator model are calculated using the blade element theory, which utilizes sectional airfoil data along with the induced velocity obtained from lower-order methods like momentum theory (i.e., one-way coupling) or the local flow velocity computed in the simulation (i.e., two-way coupling) (Ref. 2). The use of actuator models significantly reduces the computational cost (since a blade-resolved mesh is not needed) and, at the same time, can accurately capture the primary flow features (Ref. 3). Recently, Chopra et al. (Ref. 4) utilized two-way coupled actuator model to study an isolated rotor in descent and compared it with the results obtained from blade resolved simulation.

In this study, the two high-fidelity approaches of ALM-based LES (referred to as ALM-LES henceforth) and

Presented at the Vertical Flight Society's 78th Annual Forum & Technology Display, Fort Worth, Texas, USA, May 10-12, 2021.

blade-resolved DES (referred to as BR-DES) will be utilized to study a two-rotor system in forward flight. The BR-DES approach is extensively used in literature for multi-rotorcraft studies in forward flight (e.g., see Refs. 5–8) due to its capability to capture both the boundary layer flow over the blades and detailed wake structures/dynamics. On the other hand, actuator models have shown promising prospects in analyzing an isolated rotor in forward flight (Refs. 9, 10). The current study uses actuator line model for a multi-rotor configuration. This will aid in understanding how well an actuator line model can perform in a system with complex three-dimensional aerodynamic phenomenons such as blade-vortex interactions, vortex-vortex interactions, and rotor-induced turbulence onto other rotors. This paper focuses on a rotor-rotor case studied using BR-DES in Healy et al. (Ref. 8) and compare the BR-DES results with those obtained from the current ALM-LES method.

NUMERICAL METHODOLOGY

The numerical flow simulations presented in this study are conducted using a parallel stabilized finite element-based flow solver for BR-DES (Ref. 8) as well as ALM-LES (Ref. 11) that uses LES formulation presented in 12. The BR-DES approach used is described in detail in previous studies (e.g., see Ref. 8) while ALM-LES for rotors is described below (also see 4).

Actuator Line Model (ALM)

For this study, the ALM is implemented in the LES framework. The current ALM approach is described in this section. Each rotor blade is modeled as an actuator line. The loads over actuator lines are applied as volumetric source terms over a region defined around the actuator lines/blades at any given instance. Specifically, the normal and tangential forces are applied which are obtained from blade element theory (BET) using the local induced velocity as follows (note that z coordinate is normal to the rotor plane while x and y coordinates are in the rotor plane):

$$\begin{gathered}
V_{ax} = V_z \ \ \& \ \ V_t = \Omega R - \frac{xV_y - yV_x}{\sqrt{V_x^2 + V_y^2}} \\
V_{rel} = \sqrt{V_{ax}^2 + V_t^2} \ \ \& \ \ \phi = tan^{-1}(V_{ax}/V_t) \\
\alpha = \theta - \phi \\
\implies C_l(\alpha) \ \ \& \ \ C_d(\alpha) \ \ \text{(Using airfoil tables)} \\
F_L = \frac{1}{2}\rho V_{rel}^2 C_l c \ \ \& \ \ F_D = \frac{1}{2}\rho V_{rel}^2 C_d c \\
F_N = F_L cos(\phi) - F_D sin(\phi) \ \ \& \ \ F_T = F_L sin(\phi) + F_D cos(\phi)
\end{gathered} \tag{1}$$

The flow solver uses an initial set of forces calculated using the blade element momentum theory (BEMT) for a certain number of revolutions until the initial transients are passed. After this, the new set of forces are calculated using the local axial and tangential velocities based on the computed flow field. It is important to note that the forces obtained from the above equations are sectional forces. For these forces to be applied as volumetric source terms in the simulation, a region is defined around the actuator lines at any given instance. The width of this region is typically chosen to be on the order of blade chord (c). Specifically, the normal and tangential forces are smeared over a width of, $2\gamma = 2c$, in both the azimuthal (θ) and axial (z) directions. In this study, this width is kept fixed along the entire span of the blade. In summary, F_n and F_t are used to form BET-based sectional force vector $\mathbf{f_{1D}}^{BET}(r)$ and in-turn to compute the volumetric source term $\mathbf{f_{3D}}^{CFD}$ (i.e., force per unit volume) as follows:

$$\mathbf{f_{3D}}^{CFD} = \mathbf{f_{1D}}^{BET}(r)\delta(z)\delta(\theta)$$

where the following cubic spline distribution kernel (for $|z| \leq \gamma$) with a unit area is used:

$$\begin{aligned}
t_0 = \frac{z+\gamma}{\gamma}; \quad \delta(z) = \frac{1}{\gamma}\Big[-2t_0^3 + 3t_0^2\Big]; \quad z < 0 \\
t_0 = \frac{z}{\gamma}; \quad \delta(z) = \frac{1}{\gamma}\Big[2t_0^3 - 3t_0^2 + 1\Big]; \quad z \geq 0
\end{aligned}$$

Problem Setup

For this study, two in-line fixed-pitch rotors (which are representative of an eVTOL rotor (Ref. 8)) operating in forward flight are chosen. The front rotor spins clockwise and the aft rotor spins counterclockwise at the same rotational speed. Rotor hubs are positioned in-line with the free-stream since many large UAM utilize a dedicated propeller for propulsion. The rotor hubs have a longitudinal separation distance of 2.5R with no vertical separation. The blades are twisted and untapered with rectangular planform. More details about the rotor properties can be found in Table 1. The computational domain has a size of 75R x 50R x 50R in x (streamwise), y (lateral), and z (axial) directions, respectively, with the reference point being the mid-point between the two rotors as shown in Fig. 1. The inflow condition is a uniform streamwise velocity of 15.43 m/s. A no-penetration condition is set at the four side surfaces along with a traction-free/slip condition. The outlet is prescribed as zero natural pressure condition.

ALM-LES is based on the incompressible Navier–Stokes equations and utilizes the residual-based variational multiscale (RBVMS) method (Ref. 12). For BR-DES, Altair's HyperWorks CFD AcuSolve flow solver is used with the Spalart-Allmaras (SA) model for the on-body/near-body region and a static LES-type subgrid-scale model for the off-body region. Both ALM-LES and BR-DES utilize the second-order implicit time integration scheme of the generalized-α method (Ref. 13). A timestep size corresponding to 2° rotation of the blade is used for ALM-LES and 1° for BR-DES. These were found to be appropriate for the current case.

The mesh for both the approaches is kept the same in the wake and is shown in Fig. 2. For ALM-LES, the rotor region

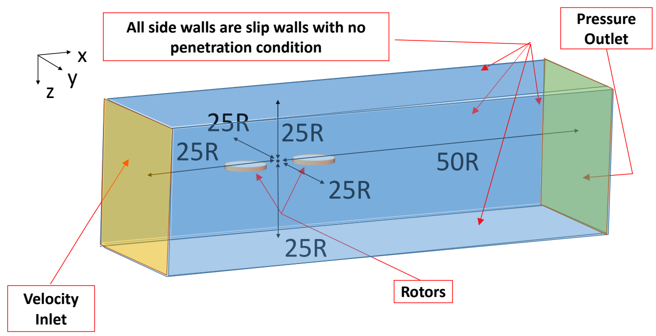

Figure 1: **Computational domain with dimensions referenced from center of two rotor system and description of boundary conditions**

Parameter	Specification
No. of blades	3
Diameter	1.6764 m
Solidity	0.076
Root Cutout	0.2R
Airfoil	NACA 23012
Twist	-10°
Root Pitch	20°
Disk Loading	239.49 N/m^2
Chord	0.0834 m
RPM	167.55 rad/s
Forward Flight Speed	15.43 m/s
Advanced Ratio	0.1

Table 1: **Rotor parameters**

uses a mesh size of $c/4$ in the x-y plane and $c/8$ in the z-direction. The total number of elements in the mesh are 29.5 million with 0.75 million elements in each rotor region. For BR-DES, on each blade, the surface mesh is set to ensure 200 elements around the airfoil, with refinement along the leading and trailing edges (0-10% and 90-100% chord, respectively). In the boundary layer mesh, the first element height is set to ensure that it is less than or equal to 1 in wall units, i.e., $\Delta y_0^+ \leq 1$. The boundary layer mesh is used until the last layer size is within 80% of the local off-body element size. The BR-DES mesh includes 120 million elements, with 48 million in each rotor region.

All simulations performed in this paper utilize the high-performance computing (HPC) systems that are part of the Rensselaer's Center for Computational Innovation (CCI).

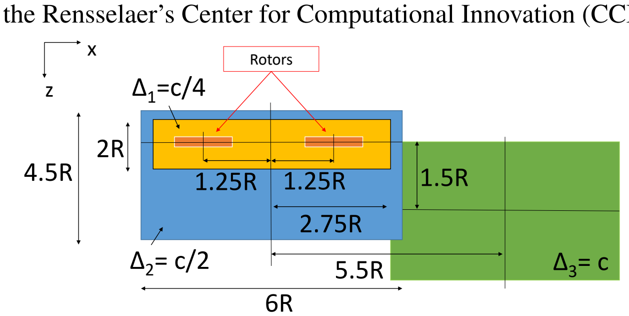

Figure 2: **Mesh setup around rotor and in wake**

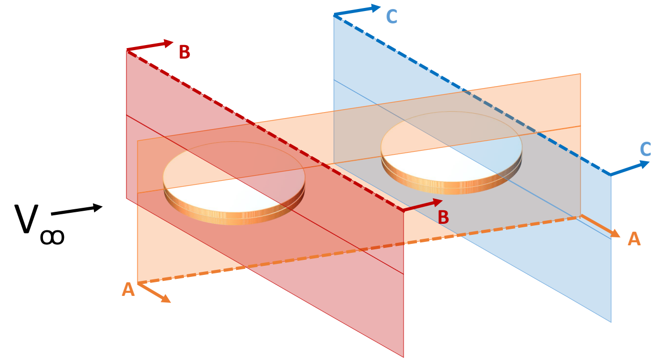

Figure 3: **Reference planes used in discussion**

ALM-LES used 2.3 GHz AMD EPYC processors and BR-DES used 2.6 GHz Intel Xeon E5-2650 processors. The goal of the paper is to showcase that ALM-LES can save on computational time when compared to BR-DES. Tab. 2 shows that ALM-LES can save computational effort by up to ~100X.

	ALM-LES	BR-DES
Total Mesh	29.5 million	120 million
Time Step	2°	1°
CPU time	296 CPU-hr/rev	24685 CPU-hr/rev

Table 2: **Summary of simulations**

RESULTS AND DISCUSSION

This section will discuss the flow field results of a two-rotor configuration in forward flight condition obtained using BR-DES and ALM-LES. Fig. 4 depicts the 3D flowfield generated by both approaches using iso-surfaces of Q-criterion colored by streamwise vorticity. Both approaches have similar wake vortex structure characterized by a large-scale two-vortex rollup system initiating from the front rotor on the advancing side (in blue) and on the retreating side (in red) (Ref. 14). Another important feature captured by both methods is the set of smaller vortex structures in between the two large rolled-up vortices. These are created by tip vortices of different intensities and opposite sign originating at $\psi = 0°$ and $\psi = 180°$. These secondary structures, that wrap around the two-vortex rollup system, are more prominent and preserved in ALM-LES than BR-DES. Looking at the wake of the aft rotor, the primary two-vortex rollup structure isn't observed but secondary vortices can be seen to convect downstream and interact with the wake from the front rotor. This wake-wake interaction leads to a breakdown of the roll-up vortices, particularly in the ALM-LES approach.

Fig. 5 shows the integrated thrust over a revolution predicted by both ALM-LES (red) and BR-DES (blue) for front rotor (solid) and aft rotor (dashed). Both approaches predicted higher thrust for front rotor compared to aft rotor. For front rotor, the difference in averaged thrust between ALM-LES

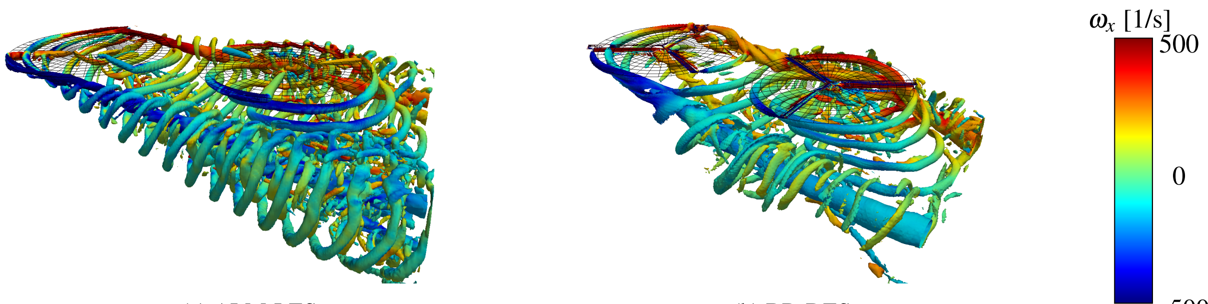

(a) ALM-LES

(b) BR-DES

Figure 4: **Isosurfaces of Q-criterion colored by stremwise vorticity. Inflow direction is from top left to bottom right.**

and BR-DES is 2.39%, though the peak-to-peak amplitude predicted by ALM-LES is 3.40% higher than BR-DES. For aft rotor, the difference in averaged thrust between ALM-LES and BR-DES is 4.29%. Unlike front rotor, the peak-to-peak amplitude is higher for BR-DES than ALM-LES by 7.60%. Note that all percentage differences mentioned above are relative to the BR-DES data.

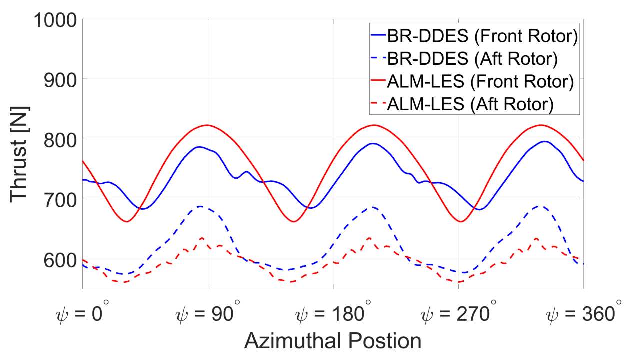

Figure 5: **Time history of integrated thrust over a revolution for front and aft rotor as predicted by BR-DES and ALM-LES**

Based on the overall flowfield and integrated thrust, the differences, though less, exist between results obtained from ALM-LES and BR-DES. Next, individual rotor behaviour is studied in-depth to understand the differences in results from ALM-LES and BR-DES.

Front Rotor Analysis

For front rotor, though the global flow physics showed similar behaviour from both ALM-LES and BR-DES as well as the average of integrated thrust are close, there are differences in amplitude between the two method. To analyze this further, Fig. 6a shows the disk plots of front rotor's sectional thrust from both approaches. Both approaches show a region of high thrust in advancing side of rotor at the outboard portion of the blade for $\psi = 90° - 180°$. For ALM-LES, the area of high thrust in this region is larger compared to BR-DES, which diffuses to lower values of thrust quickly. This difference is evident at around $\psi = 80° - 100°$, where ALM-LES shows relatively higher thrust near the tip of the blade and relatively lower thrust at $r/R = 85\%$. In retreating side of rotor, at around $\psi = 300°$, both approaches predict region of lower thrust. However, at $\psi = 270°$, significant discrepancies exist between two methods. ALM-LES shows a small region of higher thrust whereas BR-DES shows loss of thrust in that region.

To clearly highlight the differences between the two approaches, Fig. 6b shows the disk plot with difference in front rotor's sectional thrust from ALM-LES and BR-DES. Note, negative values (highlighted with blue) depicts higher thrust predicted by ALM-LES than BR-DES and positive values (highlighted by red) depicts higher thrust predicted by BR-DES. The difference disk plot shows three major areas of differences. Two of them, as discussed above, are regions at $\psi = 90°$ and $\psi = 270°$ (blade is aligned perpendicular to the flow). The third region is a band of blue (higher section thrust from BR-DES as compared to ALM-LES) that runs in the forepart of the rotor from $\psi = 120° - 240°$ at the midboard section of the blade and is not evident in Fig. 6a. We will first analyze this band in detail and then analyze the regions at $\psi = 90°$ and $\psi = 270°$.

The band seen in Fig. 6b from $\psi = 120° - 240°$ can be associated with blade-vortex interaction (BVI) taking place. An instantaneous contour of Q-criterion is shown in Fig. 7 that shows that indeed there is a BVI event taking place in and around the same region of the band which is captured by both approaches.

BVI is predicted by both the approaches, however, the band in Fig. 6b could possibly arise due to two reasons: location of vortex from rotor plane or strength and shape of vortex. These are analyzed in Fig. 8. Fig. 8b shows the overlay of Q-criterion at an instance in time captured by two approaches. It can be seen that both the vortices have a similar location in the 3D space. Fig. 8c and 8d zooms into the youngest trailed vortex, generated by ALM-LES and BR-DES respectively, cut by a plane which is colored by vortex magnitude. These figures show that both the strength of vortex and shape of it are different between two approaches. ALM-LES predicts a tighter vortex with core showing a region of high vorticity. In contrast, the vorticity in the vortex core predicted by BR-DES is significantly less

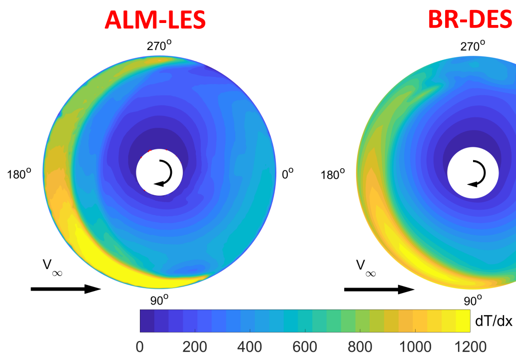

(a)

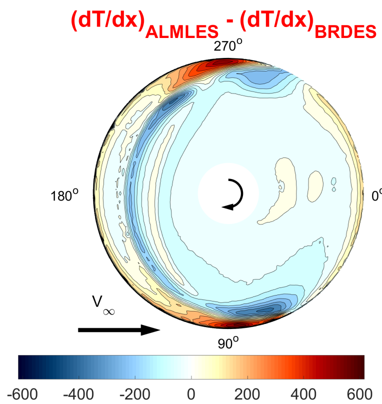

(b)

Figure 6: **Disk plots of sectional thrust (dT/dx) for front rotor. a) Absolute dT/dx by ALM-LES (left) and BR-DES (right). b) Difference in dT/dx between ALM-LES and BR-DES**

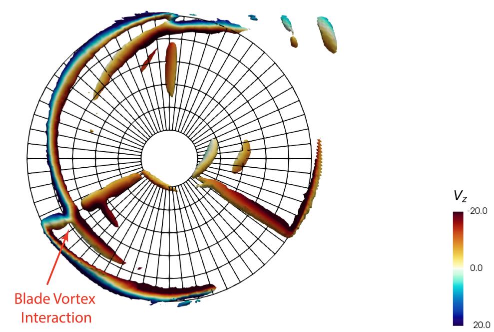

(a) **ALM-LES**

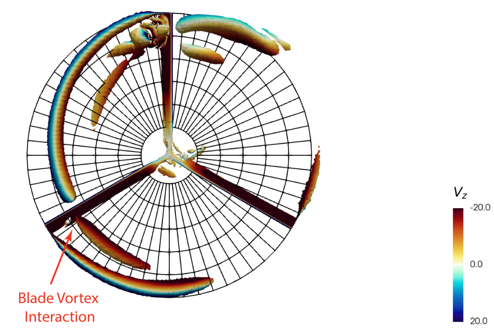

(b) **BR-DES**

Figure 7: **Top view of front rotor with isosurfaces of Q-criterion colored with velocity normal to rotor plane (V_z). Positive value (red) means velocity going into the plane and negative value (blue) means velocity coming out of plane.**

and the vortex is more diffused compared to the one in ALM-LES. Due to ALM-LES predicting a tighter shape of vortex, the strength of vortex is higher. On one side of the vortex, it leads to a region of higher downwash, compared to BR-DES, thereby high inflow angle (see Eq. 1). Higher inflow angle contributes to lower angle of attack and thus lower thrust. This lower thrust in ALM-LES is what causes the blue band. On the other side of the vortex, there is a small region of upwash which causes the ALM-LES thrust to increase slightly.

To help understand the differences between ALM-LES and BR-DES at $\psi = 90°$ and 270°, Fig. 9 is shown with iso-surface of Q-criterion along with B-B plane (see Fig. 3) colored by velocity normal to rotor plane. It can be seen from the figures that the BVI is contributing here as well to create the differences between two approaches. For instance in Fig. 9a and 9b, at the region inboard of the tip of the blades ($r/R =$ 85%), both approaches predict a region of high downwash. Recall that ALM-LES, based on BET for force calculation, utilizes the local velocity and hence sees a lower thrust as compared to BR-DES. On moving further to the tip, right at the location where vortex hits the blade (depicted by the gap or white region) there is a region of velocity very close to zero. This primarily can affect the axial velocity

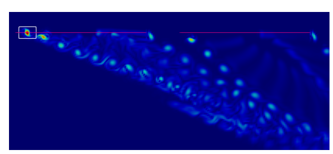

(a)

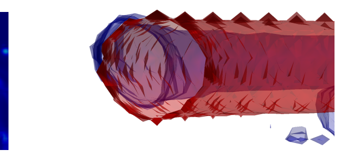

(b)

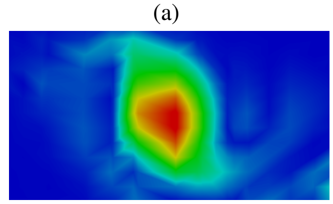

(c)

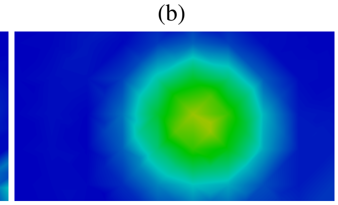

(d)

Figure 8: **Side view of flowfield normal to Plane A-A (refer to Fig. 3). a) Depiction of the focused area. b) Q-criterion to verify the location/position of vortices captured by two approaches. The red contour is from BR-DES and blue contour is from ALM-LES. c) Vortex magnitude from ALM-LES. d) Vortex magnitude from BR-DES**

(V_{ax}) which is very small compared to tangential velocity (V_{tan}) as it is governed by ΩR term. This leads to very low inflow angle and thereby high angle of attack which leads to higher lift and eventually higher thrust. This is evident in Fig. 6b at $\psi = 90°$ and near the very tip, there is a region of red, i.e., ALM-LES is predicting higher thrust than BR-DES at the same location. A similar evidence is seen in the retreating side at $\psi = 270°$ with the red region being more broader.

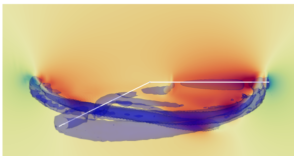

(a) **ALM-LES (blade at** 90°)

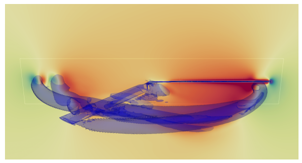

(b) **BR-DES (blade at** 90°)

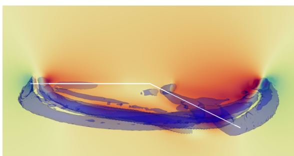

(c) **ALM-LES (blade at** 270°)

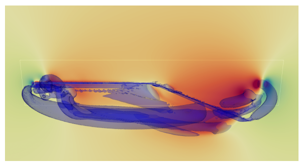

(d) **BR-DES (blade at** 270°)

Figure 9: **Front view of front rotor with isosurfaces of Q-criterion plotted with Plane B-B (refer to Fig. 3) colored by velocity normal to the rotor plane V_z. The figure is at an instance when a blade (shown by white line in case of ALM-LES) is along a certain azimuthal position.**

These differences between the two approaches could be due to the following reasons - 1 rotor loading, 2 tip-correction model, and 3 blade/vortex modeling. Since the thrust between two approaches are similar so 1 gets eliminated.

ALM-LES results are obtained without using a tip-correction model. To analyze 2, ALM-LES is performed with a tip-correction model and compared to ALM-LES without a tip-correction model, see Fig. 10. The figure confirms that the tip-correction model plays an insignificant role towards the differences between ALM-LES and BR-DES, hence 2 can also be eliminated. On analyzing 3, there is a fundamental difference on how blade is modeled and vortex is generated or interacts. The BR-DES due to physical presence of blade causes diffusion of the vortex. Whereas, in the case of ALM-LES, having no physical blade, the vortex is not only intact but also stronger. Further during interaction, there could be instances when the actuator points, where induced velocity are obtained and further calculation of forces takes place, fall in the strong viscous core region of where velocities are reaching zero or even in boundaries of vortex where velocities are very high. Hence, 3 is the strongest reason for the difference and also evident from above discussions.

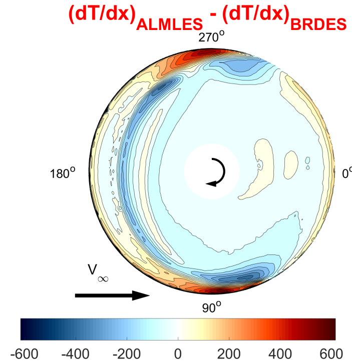

(a) **Without tip correction**

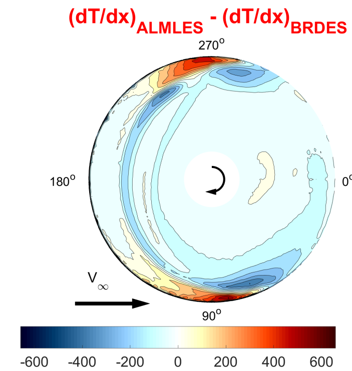

(b) **With tip correction**

Figure 10: **Disk plots of difference in sectional thrust (dT/dx) between ALM-LES and BR-DES for front rotor**

Aft Rotor Analysis

It is observed in Fig. 5 that for aft rotor there was a difference in the integrated thrust between the two approaches. We will focus on understanding the cause of such differences. Note that aft rotor is counter rotating to the front rotor. Fig. 11a shows the disk plot of sectional thrust for aft rotor captured by ALM-LES and BR-DES. Due to the wake of the front rotor, a downwash is induced in the front of the aft rotor which leads to decrease in thrust. Compared to the front rotor, the region of high thrust observed earlier in the azimuthal direction, i.e., at $\psi = 90°$. Further, the magnitude of thrust is significantly lower compared to front rotor. These two observations are consistent between both the approaches. However, there is a quantitative difference in magnitude of thrust in this region between both approaches with ALM-LES predicting a lower thrust as shown in Fig. 11b.

Fig. 12 shows the isosurfaces of Q-criterion. It is evident that the local flow field around aft rotor is affected by the front rotor. The vortex rollup from advancing side of front rotor deviates much further lower the rotor plane compared to vortex rollup from retreating side of front rotor. The reason for such a tilt is because front rotor experiences relatively higher thrust in the advancing side. Both approaches predict this tilt phenomenon. It is also evident that in ALM-LES the secondary vortices wrapping the primary rollup are more prominent, distinct, and coherent, while in BR-DES they are diffused and unstable. Further, in the case of ALM-LES, these vortices interact with the blade in the advancing side of aft rotor and causes loss of thrust which leads to above-mentioned difference between the two methods.

Similar to front rotor, the strength of vortices in the wake of aft rotor predicted by BR-DES seems lower compared to ALM-LES. For instance, the right vortex rollup originating from retreating side of front rotor has significantly lower vortex strength in case of BR-DES as compared to ALM-LES. This brings up an interesting observation that in both approaches even though the mesh and model (LES) is the same, BR-DES showcases a more diffused vortex structure in the wake. Another observation that is evident is the vortex breakdown which is more prominent in ALM-LES but not so much in BR-DES. These observations points to the difference between LES models employed by both approaches. BR-DES uses a static subgrid-scale model whereas ALM-LES employs the RBVMS model. The effect of these models will be analyzed in the future.

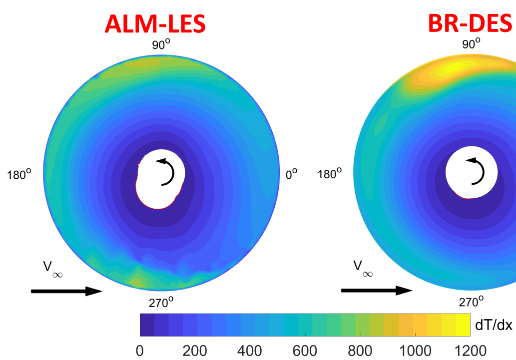

(a)

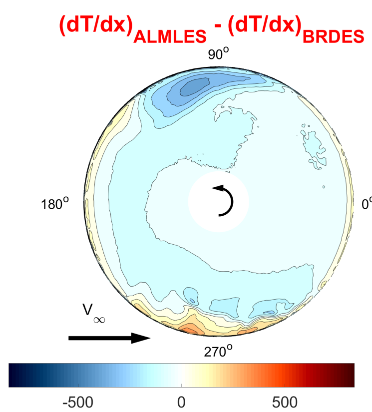

(b)

Figure 11: **Disk plots of sectional thrust (dT/dx) for aft rotor. a) Absolute dT/dx by ALM-LES (left) and BR-DES (right). b) Difference in dT/dx between ALM-LES and BR-DES**

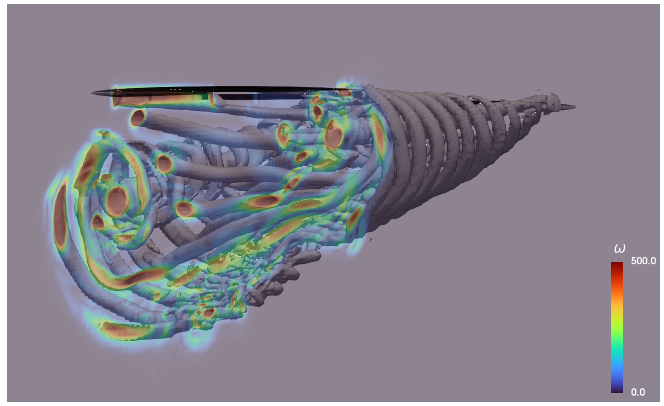

(a) **ALM-LES**

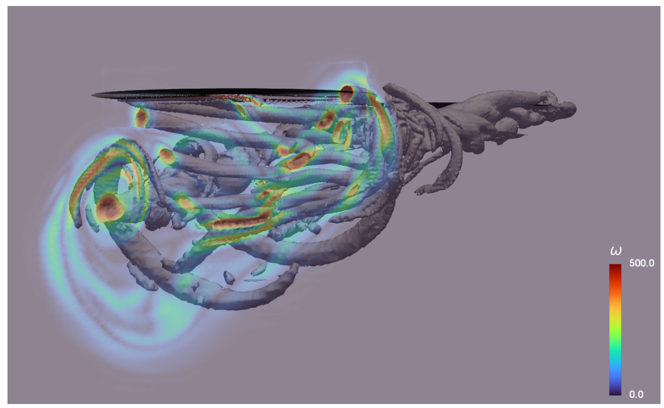

(b) **BR-DES**

Figure 12: **Isosurface of Q-criterion viewed from behind the aft rotor plotted along with Plane C-C (refer to Fig. 3) colored by vorticity magnitude (1/s).**

CONCLUSION

This study investigated the impact of different high-fidelity approaches on the interactional aerodynamics of a counter rotating two-rotor system in an edgewise flight. Flow simulations were performed using blade-resolved DES (i.e., BR-DES), and actuator line model/ALM-based LES (i.e., ALM-LES). It was done for a three-bladed rotor with a rectangular planform and linear twist, and corresponds to a large eVTOL rotor. Through these simulations, the following observations were made:

1. The global flow field is dominated by a two-vortex rollup system initiated from the front rotor that interacts with the aft rotor. These front rotor wake structures are captured similarly by the two approaches.
2. The integrated thrust from the two approaches shows good agreement, with a difference of 2.4% for front rotor and 4.3% for aft rotor. The differences are more pronounced for peak-to-peak thrust with a difference of 3.4% and 7.6% for front and aft rotor, respectively.
3. Despite wake structure agreement between the two cases, sectional thrust differences are observed in areas

with blade-vortex interaction. Due to the differences in how the blades are modeled between the two approaches, trailed vortex interactions with the blade result in differences in thrust. In case of ALM-LES, the use of BET and 2D airfoil tables for actuator points in the vicinity of vortex caused the highs and lows in the thrust which was not seen in case of BR-DES.

4. Similar to front rotor, the aft rotor showed qualitative flow-field agreement but also some blade loading differences. The differences in thrust here arose due to the interaction of secondary vortices (wrapping the vortex rollup from front rotor) with the rotor plane. Thrust differences are tied to the use of BET and 2D airfoil tables in ALM-LES and how they react to secondary vortices.

5. The vortex system that is generated by BR-DES is more diffused than ALM-LES. Furthermore, the phenomenon of vortex breakdown is encountered around the aft rotor which is more prominent in ALM-LES. This is associated with the nature of LES model used. Further analysis is needed on this aspect.

6. Overall both approaches show a good agreement for both front and aft rotors, however, some differences are also observed between the two approaches. These differences are present at certain locations of complex aerodynamic interactions. However, the computational advantage that ALM-LES gives over BR-DES is found to be significant, e.g., up to 100x.

REFERENCES

1. Sanderse, B., der Pijl, S. V., and Koren, B., "Review of Computational Fluid Dynamics for Wind Turbine Wake Aerodynamics," *Wind Energy*, Vol. 14, (7), 2011, pp. 799–819.

2. Sorensen, J. N., and Shen, W. Z., "Numerical Modeling of Wind Turbine Wakes," *Journal of Fluids Engineering*, Vol. 124, (2), 2002, pp. 393–399.

3. Stevens, R. J., Martínez-Tossas, L. A., and Meneveau, C., "Comparison of Wind Farm Large Eddy Simulations using Actuator Disk and Actuator Line Models with Wind Tunnel Experiments," *Renewable Energy*, Vol. 116, 2018, pp. 470–478.

4. Chopra, A., McCauley, J., Healy, R., Gandhi, F., and Sahni, O., "A Comparison of High-Fidelity Simulation Approaches for eVTOL Rotor Flows in Descent Conditions," 77th Vertical Flight Society Annual Forum, 2021.

5. Chaderjian, N. M., "Navier-Stokes Simulation of UH-60A Rotor/Wake Interaction using Adaptive Mesh Refinement," 73rd AHS International Annual Forum & Technology Display, 2017.

6. Misiorowski, M., Gandhi, F., and Anusonti Inthra, P., "Computational Analysis of Rotor-Blown-Wing for Electric Rotorcraft Applications," *AIAA Journal*, 2020, pp. 1–12.

7. Healy, R., Misiorowski, M., and Gandhi, F., "A Systematic CFD-Based Examination of Rotor-Rotor Separation Effects on Interactional Aerodynamics for Large eVTOL Aircraft," 75th Vertical Flight Society (VFS) Annual Forum, 2019.

8. Healy, R., Gandhi, F., and Mistry, M., "Computational Investigation of Multirotor Interactional Aerodynamics with Hub Lateral and Longitudinal Canting," *AIAA Journal*, 2021, pp. 1–11.

9. Kim, T., Oh, S., and Yee, K., "Novel Actuator Surface Method for Helicopter Rotor Analysis," *Journal of Aircraft*, Vol. 53, (6), 2016, pp. 1947–1952.

10. Linton, D., Widjaja, R., and Thornber, B., "Actuator Surface Model with Computational Fluid Dynamics Convected Wake Model for Rotorcraft Applications," *AIAA Journal*, 2021, pp. 1–15.

11. Hebbar, U., Rane, J. D., Gandhi, F., and Sahni, O., "Analysis of Interactional Aerodynamics in Multi-Rotor Wind Turbines using Large Eddy Simulations," AIAA Scitech 2020 Forum, 2020.

12. Tran, S., and Sahni, O., "Finite Element-based Large Eddy Simulation using a Combination of the Variational Multiscale Method and the Dynamic Smagorinsky Model," *Journal of Turbulence*, Vol. 18, (5), 2017, pp. 391–417.

13. Jansen, K. E., Whiting, C. H., and Hulbert, G. M., "A generalized-α method for Integrating the Filtered Navier–Stokes Equations with a Stabilized Finite Element Method," *Computer Methods in Applied Mechanics and Engineering*, Vol. 190, (3-4), 2000, pp. 305–319.

14. Caprace, D.-G., Chatelain, P., and Winckelmans, G., "Wakes of Rotorcraft in Advancing Flight: A Large-Eddy Simulation Study," *Physics of Fluids*, Vol. 32, (8), 2020, pp. 087107.